Carbohydrate Polymers 107 (2014) 72–84

Contents lists available at ScienceDirect

Carbohydrate Polymers

journal homepage: www.elsevier.com/locate/carbpol

Preparation and characterizations of solid/aqueous phases inclusion complex of 2,4-dinitroaniline with β-cyclodextrin

Thambusamy Stalin[a,*], Krishnan Srinivasan[a], Krishnamoorthy Sivakumar[b], S. Radhakrishnan[c]

[a] Department of Industrial Chemistry, School of Chemical Sciences, Alagappa University, Karaikudi 630 003, Tamil Nadu, India
[b] Department of Chemistry, Sri Chandrasekharendra Saraswathi Viswa Mahavidyalaya University, Enathur, Kanchipuram 631 561, Tamil Nadu, India
[c] Central Electrochemical Research Institute, Karaikudi 630 006, Tamil Nadu, India

ARTICLE INFO

Article history:
Received 31 October 2013
Received in revised form 24 January 2014
Accepted 28 January 2014
Available online 5 February 2014

Keywords:
β-Cyclodextrin
2,4-Dinitroaniline
Inclusion complex
2D ROESY NMR
Patch dock server

ABSTRACT

The formation of host–guest inclusion complex of 2,4-dinitroaniline (2,4-DNA) with nano-hydrophobic cavity of β-cyclodextrin (β-CD) in solution phase were studied by UV–visible spectrophotometer and electrochemical method (Cyclic Voltammetry, CV). The prototropic behaviors of 2,4-DNA with and without β-CD was studied by spectrophotometrically. The binding constant of the inclusion complex at 303 K was calculated using Benesi–Hildebrand plot and thermodynamic parameter (ΔG) were also calculated. The inclusion complex formation between β-CD and 2,4-DNA was confirmed by ^{1}H NMR, 2D ROESY NMR, FT-IR, XRD and SEM analysis. The 2,4-DNA:β-CD inclusion complex was obtained by molecular docking studies and it was good correlation with the results obtained through experimental methods.

1. Introduction

Cyclodextrins (CDs) are cyclic oligosaccharides consisting of 6, 7, and 8 units of 1,4-linked glucose units, and are named alpha (α), beta (β) and gamma (γ)-Cyclodextrins, respectively (Scheme 1). These macromolecules, which can be spatially represented as a torus with wide and narrow openings corresponding to secondary and primary hydroxyl groups respectively, can encapsulate a large variety of compounds due to the hydrophobic character of their internal cavity (Szejtli, 1998). Although the depth of the cavities for the three CDs is the same (~0.78 nm), their cavity diameters are ~0.57, 0.78 and 0.95 nm, respectively. Due to the unique chemical structure of CD molecules, the inner side of the cavity is hydrophobic and the outer side is hydrophilic. The hydrophobic nature of the CD cavities facilitates the ability of CDs to act as host for both nonpolar and polar guests, which include small molecules as well as polymers (Do Nascimento, Da Silva, De Torresi, Santos, & Temperini, 2002; Harada, Nishiyama, Kawaguchi, Okada, & Kamachi, 1997; Shuai, Porbeni, Wei, Shin, & Tonelli, 2001; Szejtli, 1998). Once the inclusion compound is formed, the stability of the guest molecules increases due to the binding forces (van der Waals attractions, hydrogen bonding, hydrophobic interactions, etc.) between the host (CDs) and guest molecules (Rekharsky & Inoue, 1998; Schneider, Hacket, & Rudiger, 1998). The CDs also have several advantages in other areas, such as the food, cosmetics industries and agro chemistry (Loukas, Jayasekera, & Gregoriadis, 1995; Loukas, Vraka, & Gregoriadis, 1996; Zhang, Lerner, Rustrum, & Hofman, 1999), especially owing to their capacity to protect the guest molecules against oxidation, light-induced reaction and loss by evaporation. Additionally, they usually enhance the aqueous solubility of poorly soluble or even insoluble compounds such as organic and drug molecules (Choi, Nyongryu, Ryoo, & Pillee, 2001).

2,4-Dinitroaniline (2,4-DNA), as dinitro-substituted derivatives of aromatic amines, have become more and more significant in environmental studies due to their highly toxic nature and their suspected carcinogenic properties (Dimou, Sakkas, & Albanis, 2004; Xiang, Tong, & Lin, 2007). This 2,4-DNA was mainly used as intermediates in the synthesis of dyestuff (Xifeng et al., 2006; Xu, Liu, Wu, & Feng, 2004), pharmaceuticals (Armson et al., 1999), pesticides (Ayala, El-Din, & Smith, 2010; Benbow, Bernberg, Korda, & Mead, 1998), and herbicides (Kataoka, 1996; Kearney, Isensee, & Koktson, 1977; Wang & Arnold, 2003), and they are released into the environment directly as industrial waste or indirectly as degradation products of herbicides and pesticides. After entering into the environment, this compound can experience complex environmental transformations at trace level, and it is very harmful to the environment potentially. Acute or chronic exposure to 2,4-DNA can produce symptoms of headache, dizziness and nausea.

* Corresponding author. Tel.: +91 9944266475; fax: +91 4565 225202.
E-mail addresses: tstalinphd@rediffmail.com, drstalin76@gmail.com (T. Stalin).

0144-8617/$ – see front matter © 2014 Elsevier Ltd. All rights reserved.
http://dx.doi.org/10.1016/j.carbpol.2014.01.091

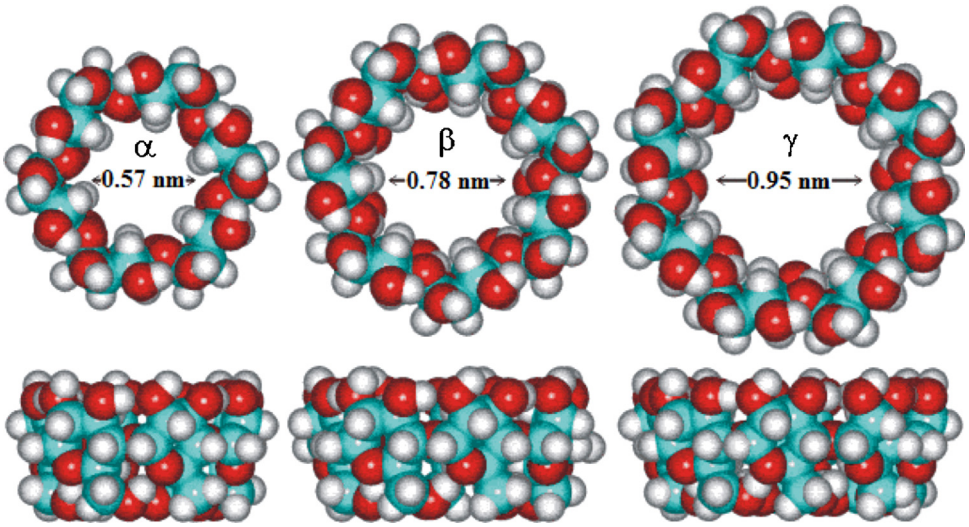

Scheme 1. 3D view of chemical structures of α-CD, β-CD and γ-CD.

With the growing use of these compounds in different industries, the 2,4-DNA have been included in the list of priority pollutants in many countries. In view of the environmental importance of separation of the 2,4-DNA present in the wastewaters, surface waters and other environments at trace level or ultra trace level. The β-CD can be used to separate this compound from aqueous medium by preparing their inclusion complex, because the β-CD can selectively include the 2,4-DNA by hydrophobic interaction. 2,4-DNA is a good candidate as a model compound to characterize inclusion formation by ^{1}H NMR and FT-IR spectroscopy.

In this present study, we report the inclusion complex formation in solution phase by UV–visible spectroscopy and cyclic voltammetric technique. The solid complex was prepared and characterized by ^{1}H NMR, 2D ROESY NMR, FT-IR, XRD, SEM techniques and molecular docking technique (using PatchDock server) in a virtual state. We found that the virtual state analysis results correlates well with the liquid and solid-state analysis results.

2. Experimental

2.1. Instruments

The UV–Vis spectra (absorption spectral measurements) were carried out with Shimadzu UV-2401PC double-beam

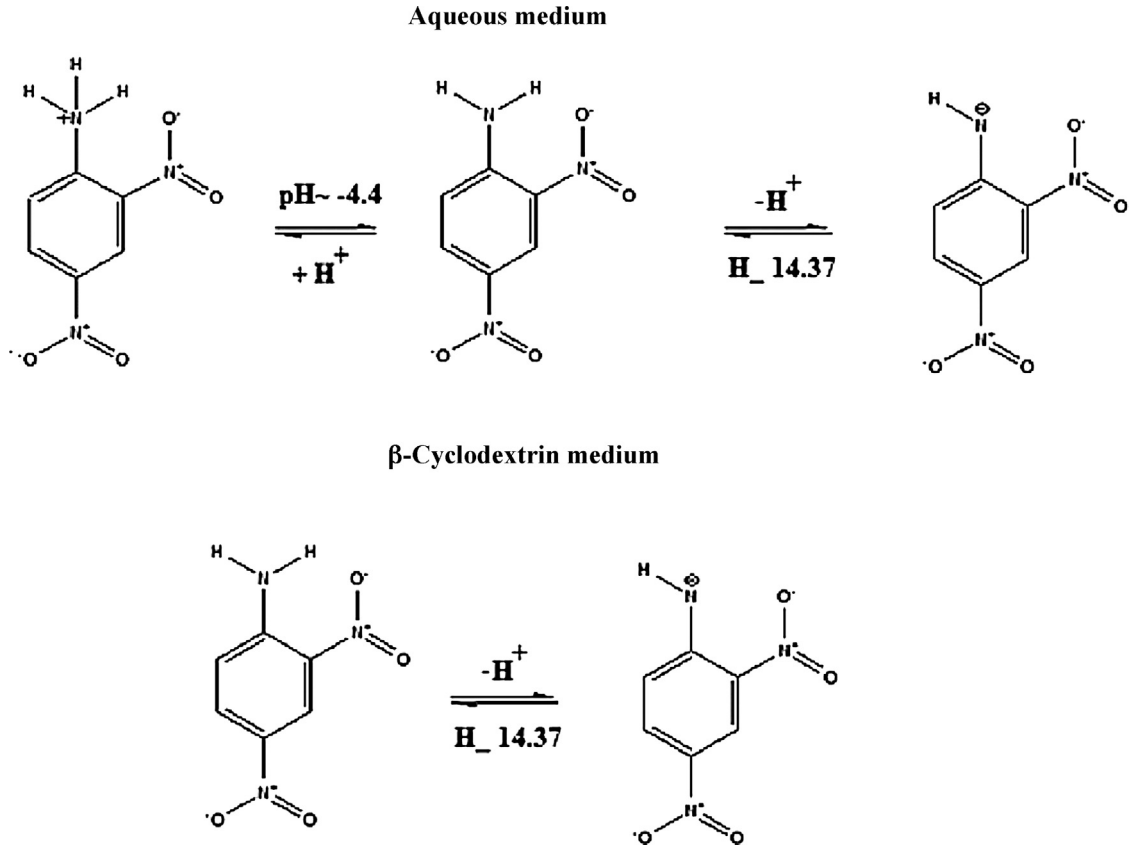

Scheme 2. Various prototropic equilibria of 2,4-DNA in aqueous and β-CD medium.

Table 1
Various prototropic maxima (absorption spectra) and pK_a values of 2,4-DNA in without and with β-CD medium.

species	Without β-cyclodextrin		With β-cyclodextrin	
	λ_{max} (nm)	pH	λ_{max} (nm)	pH
Monocation	400 (Sh)	−4.4	–	–
	348			
	233			
	206			
Neutral	348	−4.0 to 14.02	347	−4.0 to 14.02
	263		261	
	227		224	
			212	
Monoanion	516	14.37	519	14.37
	349		350	
	262		262	
	225		224	
pK_a	−4.4			

Sh – Shoulder.

spectrophotometer, the pH values in the range 2.0–12.0 were measured on Elico pH meter LI-120; Electrochemical studies were carried out using an Auto lab electrochemical analyzer, it used to apply potential on the working electrode equipped with a three-electrode glassy carbon electrode (diameter: 1 mm) serves as a working electrode system. Reference electrode was saturated calomel electrode (SCE) and platinum wire as counter electrode. All experiments were carried out at 30 ± 1 °C. The working electrode was polished to a mirror with 0.05 μm alumina aqueous slurry, and rinsed with triply distilled water before each experiment. The supporting electrolyte was pH ∼ 7 (0.1 M KH_2PO_4 + 0.1 M NaOH) and H_14.37 (2 M NaOH). ^{1}H NMR (D2O, 500 MHz) spectra were taken by BRUKER-NMR instrument operating at 300 K using a 5 mm probe. The sample solutions for ^{1}H NMR were prepared by dissolving the 2,4-DNA and its complex in D_2O solvent to obtain the final concentration of 20 mM. Two-dimensional rotating-frame Owerhauser effect spectroscopy (ROESY) experiments were performed by BRUKER-NMR 400 MHz, instrument operating at 300 K and the standard Bruker program was used, DMSO-d6 was used as a solvent, relaxation delay of 1 s and mixing time 300 ms under the spin lock conditions. Powder X-ray diffraction spectra were taken by XPert PRO PANalytical diffractometer. FT-IR was recorded using Nicolet 380 Thermo Electron Corporation Spectrophotometer using KBr pellets between 4000 and 400 cm^{-1}.

2.2. Molecular docking study

The most probable structure of the 2,4-DNA:β-CD inclusion complex was determined also by molecular docking studies using the PatchDock server (Duhovny, Inbar, Nussinov, & Wolfson, 2005). The 3D structural data on β-CD and 2,4-DNA was obtained from crystallographic databases. The guest molecule (2,4-DNA) was docked into the host molecule (β-CD) cavity using PatchDock server by submitting the 3D coordinate data of 2,4-DNA and β-CD molecules. Docking was performed with complex type configuration settings. PatchDock server follows a geometry-based molecular docking algorithm to find the docking transformations with good molecular shape complementarity. PatchDock algorithm separates the Connolly dot surface representation (Connolly, 1983a; Zhang, Vasmatzis, Cornette, & DeLisi, 1997) of the molecules into concave, convex and flat patches. These divided complementary patches are matched in order to generate candidate transformations and evaluated by geometric fit and atomic desolvation energy scoring (Connolly, 1983b) functions. RMSD (root mean square deviation) clustering is applied to the docked solutions to select the non-redundant results and to discard redundant docking structures.

2.3. Reagents

β-Cyclodextrin {(β-CD), was obtained from the Sd fine chemical company} and used without further purification. 2,4-Dinitroaniline (2,4-DNA) purchased from the SRL chemical reagents company. Triply distilled water was used to prepare all solutions. Solutions in the pH range 2.0–12.0 were prepared by adding the appropriate amount of NaOH and H_3PO_4. Yagil basicity scale (H_-) (Yagil, 1967) for solutions above pH ∼ 12 (using a NaOH–H_2O mixture) and A modified Hammett's acidity scale (H_0) (Jorgenson & Hartter, 1963) for the solutions below pH ∼ 2 (using a H_2SO_4–H_2O mixture) was employed. The solutions were prepared just before taking measurements. The concentrations of the solutions were of the order (10^{-4} to 10^{-5} mol/L). The stock solution of 2,4-DNA and β-CD preparation for spectral and electrochemical studies were prepared by adopting the procedure detailed in our previous report (Stalin, Srinivasan, Kayalvizhi, & Sivakumar, 2011; Stalin, Srinivasan, Vaheethabanu, & Manisankar, 2011).

2.4. Preparation of solid inclusion complex of 2,4-DNA with β-CD

Accurately weighed 1 g of the β-CD was placed into 100 ml conical flask and 30 ml triply distilled water added and then oscillated to completely dissolve the β-CD. After that, 0.1612 g of 2,4-DNA was put into a 10 ml beaker and 5 ml ethanol was added and put over electromagnetic stirrer to stir until it was dissolved. Then slowly poured 2,4-DNA solution into β-CD solution. The above mixed solution was continuously stirred for 48 h at room temperature. The reaction mixture was kept in to refrigerator for 48 h. At this time, a yellow precipitate was formed. The precipitate was filtered by G4 crucible and washed with triply distilled water. After drying in oven at 50 °C for 12 h, yellow powder was obtained. This is an inclusion complex of 2,4-DNA with β-CD and it further analyzed by ^{1}H NMR, 2D ROESY NMR, FT-IR, XRD and SEM analysis.

3. Results and discussion

3.1. Effect of pH

The absorption spectra of 2,4-DNA were recorded at different pH solution and the relevant data are compiled in Table 1 and Fig. 1. In the pH range 2.0–12 absorption maxima nearly resemble with the spectra observed in non-aqueous solvents (e.g. in 2-propanol at 335.5 nm, acetonitrile at 335 nm and DMF at 345 nm) and thus can be assigned to the neutral species, and also the absorption maxima was observed in aqueous medium at 348 nm, its due to the exists of the neutral form of 2,4-DNA. With a decrease in pH from 2.0, there

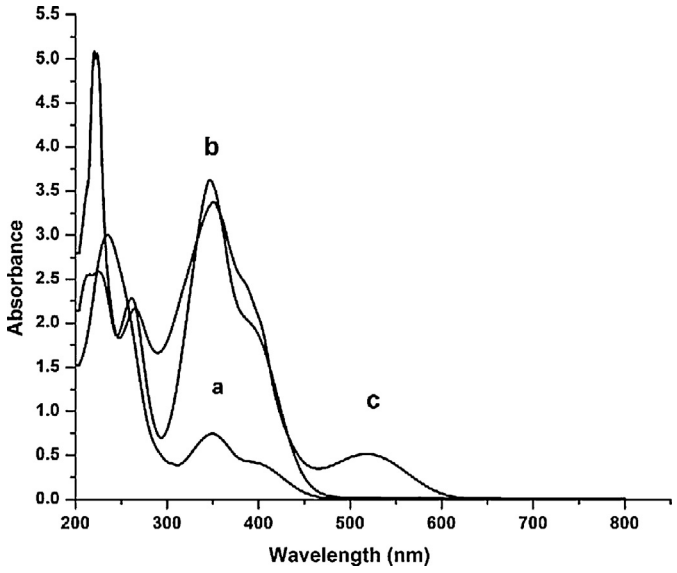

Fig. 1. Absorption spectra of different prototropic species of 2,4-DNA at 303 K; concentration 2×10^{-4} M (a) monocation (b) neutral and (c) monoanion.

is no change in the absorption maxima in higher acidic medium (up to H_0 −3.87). The absorption intensity was decreased at H_0 −4.4, also a shoulder peak was observed at 400 nm, this is due to the formation of monocation. The absorption intensity was decreases (H_0 −4.4) due to the protanation with a lone pair of electrons present on the amino group. In the case of 2,4-DNA (neutral), absorption maxima was observed at 348 nm because of the lone pair of electrons on N atom is in conjugation with the π-bond system of the benzene ring. In an alkali medium (at H_14.37), a new absorption peak was observed at 517 nm; this is due to the formation of monoanion, due to deprotanation of the aniline group. Here the more conjugation is established and the negative charge attracted by the nitro group in the para position through the benzenoid system. The prototropic equilibrium was shown in Scheme 2. The pK_a value for the equilibrium was determined spectrophotometrically (Table 1).

3.2. Effect of β-cyclodextrin

Table 2 and Fig. 2 show the absorption maxima of 2,4-DNA (2×10^{-4} mol/L) in pH ~ 7 (neutral) and H_14.37 (monoanion) solutions containing different concentrations of β-CD. At pH ~ 7, 2,4-DNA exists as a neutral form only, hence we also recorded spectra at H_14.37 as an anionic form. The absorption spectra of these two forms (neutral, monoanion) are drastically different. In pH ~ 7 and H_14.37, no clear isosbestic point was observed in the absorption spectra even in the presence of higher β-CD concentration. The equilibrium between neutral and monoanion forms of 2,4-DNA in β-CD medium.

$$\beta\text{-CD} + 2,4\text{-DNA} \underset{\text{pH}\,7}{\rightleftarrows} \beta\text{-CD} : 2,4\text{-DNA} \overset{-H^+}{\underset{\text{H\_14.37}}{\rightleftarrows}} \beta\text{-CD} : 2,4\text{-DNA}^{(-)} \quad (1)$$

In pH ~ 7 solutions the absorption intensities are increased due to the formation of an inclusion complex. In the absorption spectra of 2,4-DNA (pH ~ 7), there was no considerable spectral shift in the absorption maxima, because there is no hydrogen bond formation between β-CD and 2,4-DNA, At pH ~ 7, 2,4-DNA exist as

Table 2
Absorption maxima (nm) and log ε of 2,4-DNA at different concentrations of β-CD in H_14.37 and pH ~ 7 solutions.

S.No	Concentration of β-CD (mM)	H_14.37		pH ~ 7	
		λ_{max} (nm)	log ε	λ_{max} (nm)	log ε
1	Without β-CD	516	3.12	348	4.22
		349	4.23	263	4.03
		262	4.06	227	4.05
		225	4.36		
2	2	517	3.17	348	4.24
		349	4.21	262	4.05
		262	4.06	213	4.11
		222	4.40		
3	4	517	3.18	347	4.25
		349	4.23	262	4.05
		262	4.07	225	4.11
		226	4.39	213	4.12
4	6	517	3.19	347	4.26
		350	4.21	262	4.06
		262	4.07	224	4.10
		225	4.39	211	4.11
5	8	517	3.21	347	4.26
		350	4.23	262	4.06
		262	4.09	224	4.10
		226	4.40	212	4.11
6	10	517	3.23	347	4.26
		350	4.24	262	4.06
		263	4.06	224	4.10
		223	4.32	212	4.11
7	12	519	3.32	347	4.26
		350	4.19	261	4.06
		262	4.05	224	4.11
		224	4.31	212	4.12
Binding constant (M^{-1})		81		380	
ΔG (kJ mol^{-1})		−11		−15	

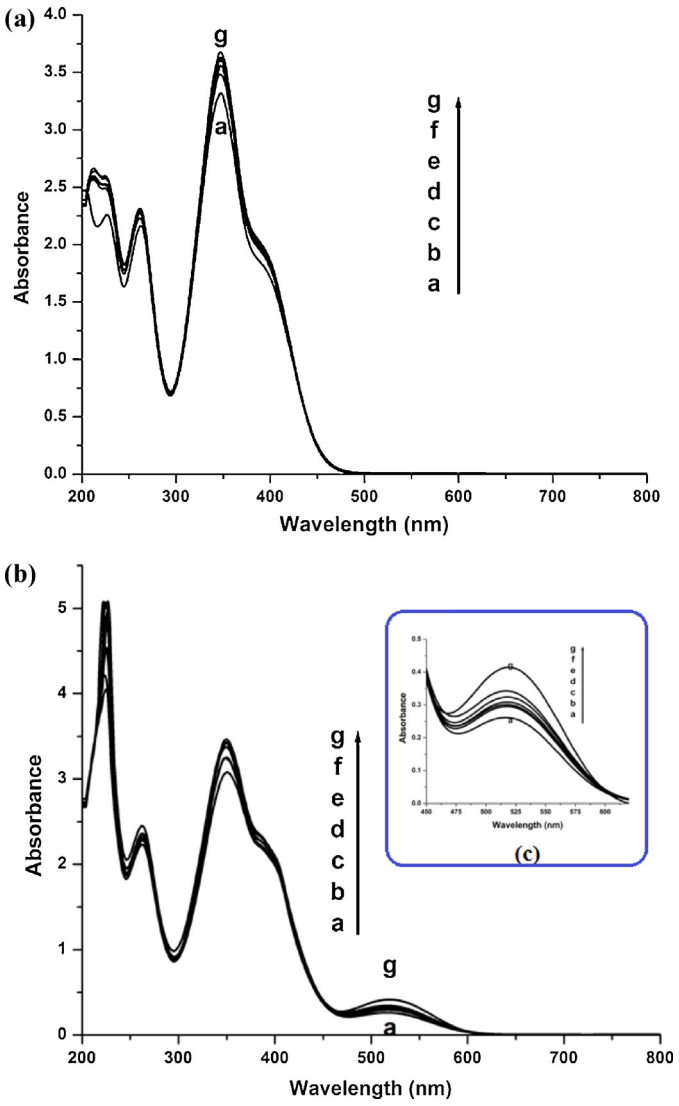

Fig. 2. Absorption spectra of 2,4-DNA (Conc. 2×10^{-4} M) in (a) pH ~ 7 and (b) H_14.37 (c) maginfication of β-CD effect solutions at different β-CD (a – g Conc. $0–12 \times 10^{-3}$ M).

the neutral form only and also 2,4-DNA located inside the β-CD cavity and the NH_2 group located at above the β-CD rim, which will cause the increase of the absorbance. In H_14.37; 2,4-DNA exist as an anionic form with formation of an inclusion complex. In H_14.37 the 2,4-DNA located inside the β-CD cavity and the $NH^{(-)}$ group located at above the β-CD rim, which will cause the increase in the absorbance intensities. In these two pH solutions (neutral and monoanion) the UV–Vis absorption behavior of the inclusion complex was same as in aqueous medium. This behavior has been attributed to the enhanced dissolution of the 2,4-DNA molecule through the hydrophobic interaction between 2,4-DNA and β-CD. These results indicate that 2,4-DNA molecule was entrapped into β-CD cavity. In both cases, the binding constant for the formation of 2,4-DNA:β-CD inclusion complex has been determined by analyzing the changes in the intensity of absorbance with the β-CD concentration. In this Fig. S1 plotting $1/(A - A_0)$ versus 1/[β-CD] for the host: guest inclusion complex and it gives straight line at pH ~ 7 and H_14.37, The binding constant (K) can be obtained by using the modified Benesi–Hildebrand equation (Benesi & Hildebrand, 1949) for the 1:1 complex Eq. (2) between 2,4-DNA and β-CD as shown below.

$$\frac{1}{A - A_0} = \frac{1}{\Delta\varepsilon} + \frac{1}{K[2,4\text{-DNA}]_0 \Delta\varepsilon[\beta\text{-}CD]_0} \quad (2)$$

where $A - A_0$ is the difference between the absorbance of 2,4-DNA in the presence and absence of β-CD, $\Delta\varepsilon$ is the difference between the molar absorption coefficient of 2,4-DNA and the inclusion complex $[2,4\text{-DNA}]_0$ and $[\beta\text{-CD}]_0$ are the initial concentration of 2,4-DNA and β-CD respectively. A good correlations were obtained (Fig. S1; $r^2 = 0.9864$ and 0.978 for pH ~ 7 & H_14.37, respectively), it confirms that the formation of the inclusion complex as 1:1 in the molar ratio. From the intercept and slope values of this plot K were calculated [pH ~ 7 = 380 M^{-1}, H_14.37 = 81 M^{-1}] at 303 K (Table 2). The determination of the thermodynamic parameter for inclusion process change in the free energy (ΔG) can be calculated from the binding constant 'K' by the following Eq. (3).

$$\Delta G = -RT \ln K \quad (3)$$

The thermodynamic parameter ΔG, for the binding of the guest molecule to β-CD cavity is given in Table 2. As can be seen from Table 2, ΔG is a negative value, which suggests that the inclusion process proceeded spontaneously at 303 K. This indicates that the formation of inclusion complex is an exergonic process.

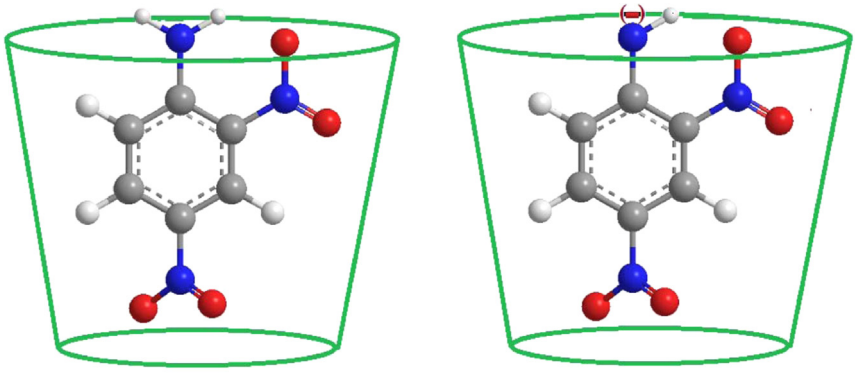

Scheme 3. The proposed structure of inclusion complex of 2,4-DNA with β-CD for 1:1 inclusion complex. The oxygen atoms are shown as red ball, nitrogen as blue and carbon as gray color balls; hydrogen atoms are white balls. (For interpretation of the references to color in this scheme legend, the reader is referred to the web version of the article.)

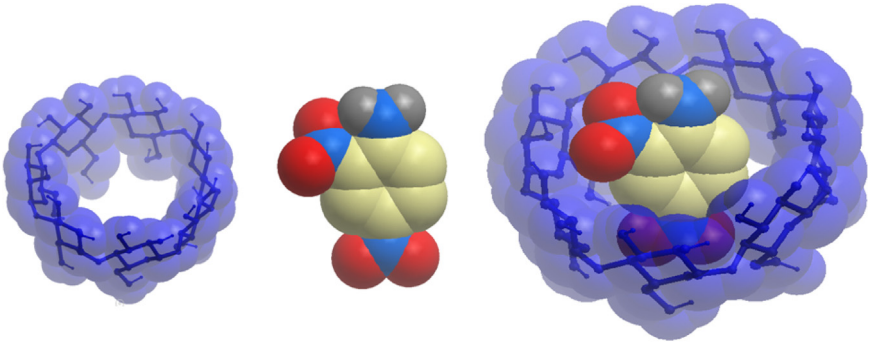

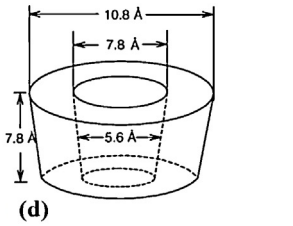

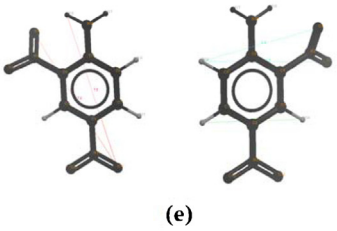

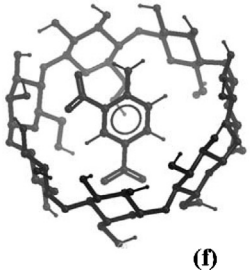

2,4-dinitroaniline bond distance in Å		Orientation
$H_{18}-O_{13}$	7.0	Vertical
$H_{17}-O_{12}$	7.0	Vertical
O_3-O_{13}	7.0	Vertical
$H_{16}-O_1$	5.6	Horizontal
$H_{15}-H_{14}$	4.3	Horizontal
$H_{16}-O_3$	4.9	Horizontal

Scheme 4. Rasmol 3D model of (a) β-CD (b) 2,4-DNA (c) 2,4-DNA:β-CD inclusion complex and bond distance of (d) β-CD, (e) 2,4-DNA and (f) 2,4-DNA:β-CD. The oxygen atoms are shown as red ball, nitrogen as blue balls. (For interpretation of the references to color in this scheme legend, the reader is referred to the web version of the article.)

3.3. Possible inclusion complex of 2,4-DNA in β-CD cavity

In 1:1 inclusion complex, the aromatic moiety was embedded in β-CD cavity and the NH_2 group present above the β-CD rim. The formation of the 1:1 host: guest complex is clearly demonstrated in Scheme 3. Such 1:1 inclusion complex structure gains further stabilization energy by releasing of water from hydrophobic cavity. In 1:1 complex, the binding constant for pH ~ 7 is considerably greater than that of in H_14.37. The binding constant is very sensitive to changes of pH values, which further supported the selective inclusion associated with the species form of 2,4-DNA. Of the two species, we should note that the β-CD can readily accept the neutral species than the anionic species, because the anionic species is more hydrophilic than the neutral species. The inclusion complex has further stabilized by the interaction of lone pair electrons of secondary hydroxyl group of β-CD with π electrons (benzenoid) of 2,4-DNA. The pH dependent changes in the absorption of the 2,4-DNA molecule in β-CD solution have also been recorded (Table 1). The formation of monoanion in β-CD medium with absorption maxima was same behavior as without β-CD medium, due to the 2,4-DNA was included into the nano hydrophobic cavity of β-CD and the $NH^{(-)}$ group present above the β-CD rim. Hence there is no more difficult to deprotonate in β-CD medium. To substantiate the above discussion, the effect of β-CD on the prototropic equilibrium, the 2,4-DNA is present as neutral in pH range −4.0 to 14.02, monoanion at H_14.37 (Scheme 2). The absorption spectra of 2,4-DNA in ground state shows the above pH (−4.0 to 14.0) as, neutral to monocation (without β-CD) are hyperchromic effect was observed only in aqueous medium and neutral to monoanion are red shifted in β-CD medium, it was similar to in aqueous medium (Scheme 2), its indicating 2,4-DNA molecule entrapped in β-CD cavity.

3.4. Molecular docking study of inclusion process

The 3D structure of β-CD and 2,4-DNA obtained from crystallographic databases are shown in Scheme 4a and b. The guest molecule, 2,4-DNA was docked into the cavity of β-CD using PatchDock server. The PatchDock server program gave several possible docked models for the most probable structure based on the energetic parameters; geometric shape complementarity score, approximate interface area size and atomic contact energy (Armson et al., 1999) of the 2,4-DNA:β-CD inclusion complex (Table 3). The docked 2,4-DNA:β-CD 1:1 model (Scheme 4c) with the highest geometric shape complementarity score 2344, approximate interface area size of the complex 245 $Å^2$ and atomic contact energy −819 kJ mol^{-1} were the highly probable and energetically favorable model and it is in good correlation with results obtained through experimental methods.

3.4.1. Semi empirical quantum mechanical calculations

The internal diameter of the β-CD is approximately 7.8 Å and its height is 7.8 Å (Scheme 4d). Considering the shape and dimensions of β-CD, 2,4-DNA can be completely embedded in the β-CD cavity. The ground state of 2,4-DNA (Scheme 4e) molecule was optimized using the AM1 method. The vertical distances between H_{17}–O_{12}, H_{18}–O_{13} and O_3–O_{13} is 7.0 Å. The horizontal distance between

Table 3
Scores of the top 10 docked models of 2,4-DNA:β-CD inclusion complex computed using PatchDock server.

Model	Geometric shape complementarity score	Approximate interface area size of the complex (Å^2)	Atomic contact energy (kcal/mol)
1	2344	245.00	−195.65
2	2330	246.30	−196.48
3	2266	237.00	−178.38
4	2234	244.50	−184.13
5	2062	233.60	−91.20
6	1978	201.90	−144.53
7	1760	238.90	−183.85
8	1708	241.30	−182.20
9	1684	237.40	−178.94
10	1560	176.90	−158.40

H_{16}–O_1 is 5.6 Å, H_{15}–H_{14} is 4.3 Å and H_{16}–O_3 is 4.9 Å The vertical distance and the horizontal distance measured from the terminal atoms of 2,4-DNA is less than the height and vertical diameter of β-CD. Since, the height of 2,4-DNA is lower than upper-lower rim of β-CD, the insertion of 2,4-DNA in the β-CD cavity is possible as shown in Scheme 4f.

3.5. Electrochemical studies

The cyclic voltammograms shows an electrochemical behavior of 2,4-DNA in pH ~ 7 and H_14.37 with β-CD (Fig. 3). Formation of the inclusion complex of 2,4-DNA with β-CD also confirmed by electrochemical method. In pH ~ 7 the cyclic voltammograms shows an anodic peak during the forward scan (toward positive potential) at −0.104 V and two reduction peaks during the reverse scan (toward negative potential) at −0.363 V and −0.775 V. These peaks are ascribed as oxidation of 2,4-DNA (NH_2; −0.104 V) and the reduction of anilinium ions (−0.363 V) into NH_2 and another one reduction peak of NO_2 (−0.775) into hydroxylamine.

In H_14.37, from the cyclic voltammograms two-reduction peak was observed during the reverse scan (toward negative potential) at −0.465 V and −0.712 V. These peaks were ascribed as reduction of $-NH^{(-)}$ into $-NH_2$ and NO_2 (−0.712 V) into hydroxylamine. The oxidation and reduction mechanism of 2,4-DNA was clearly explained in Scheme 5.

The cathodic peak current i_{pc} (Fig. 3 and Table 4) was increased with increasing the β-CD concentration in both pH solutions (pH ~ 7 and H_14.37). The cathodic peak potential, Ep_c, shifted toward a positive direction in pH ~ 7 and negative direction in H_14.37 when β-CD concentration was increased in both cases. The result showed that the inclusion complex between 2,4-DNA and β-CD was formed when 2,4-DNA was added into β-CD aqueous solution. In addition, the cathodic peak current was increased with increasing β-CD concentration; this is due to the nitro groups

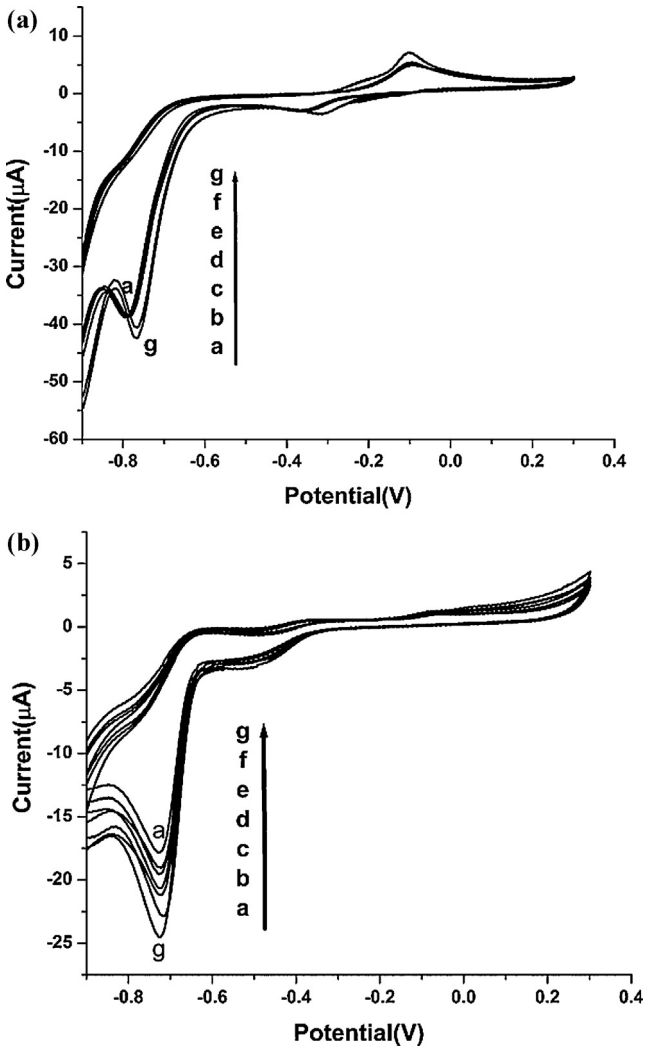

Fig. 3. CV for 2,4-DNA:β-CD in (a) pH ~ 7 and (b) H_14.37 buffer solution, scan rate 100 mV s^{-1}, 2,4-DNA (Conc. 2 × 10^{-4} M) and β-CD (a – g Conc. 0–12 × 10^{-3} M).

are encapsulated in the β-CD cavity and the catalytic behavior of β-CD to the included guest molecule (2,4-DNA).

The binding constant (K) and the stoichiometric ratio of the inclusion complex of 2,4-DNA can be determined according to the Benesi–Hildebrand (Benesi & Hildebrand, 1949) relation assuming the formation of a 1:1 host–guest complex.

$$\frac{1}{I_{HG} - I_G} = \frac{1}{\Delta I} + \frac{1}{K[2,4\text{-DNA}]_0 \Delta I[\beta\text{-CD}]_0} \quad (4)$$

Table 4
CV for 2,4-DNA:β-CD in H_14.37 and pH ~ 7 buffer solution, scan rate 100 mVs^{-1}, 2,4-DNA (Conc. 2×10^{-4} M) and (a-g) 0 –12×10^{-3} M β-CD concentrations.

Concentration of β-CD (mM)	H_14.37			pH ~ 7		
	Epc (V)	Ipc (μA)	Epa (V)	Ipa (μA)	Epc (V)	Ipc (μA)
Without β-CD	−0.465−0.712	−0.524−10.070	−0.104	6.242	−0.363−0.775	−0.808−14.260
2	−0.470−0.719	−0.608−11.140	−0.104	6.186	−0.363−0.775	−0.808−14.370
4	−0.478−0.719	−0.746−11.920	−0.102	5.780	−0.358−0.775	−1.734−14.590
6	−0.480−0.719	−0.777−11.990	−0.097	4.443	−0.356−0.775	−1.843−14.760
8	−0.482−0.719	−0.816−12.470	−0.094	4.268	−0.35 −0.761	−1.863−16.800
10	−0.492−0.719	−0.820−13.890	−0.094	4.268	−0.314−0.761	−1.912−17.500
12	−0.495−0.720	−0.988−15.380	−0.094	4.095	−0.314−0.761	−1.972−18.010
Binding constant (M^{-1})	11.8		12			
ΔG (kJ mol^{-1})	−6.2		−6.3			

Electrode reaction in pH~7 phosphate buffer

Oxidation (scaning towards positive potential)

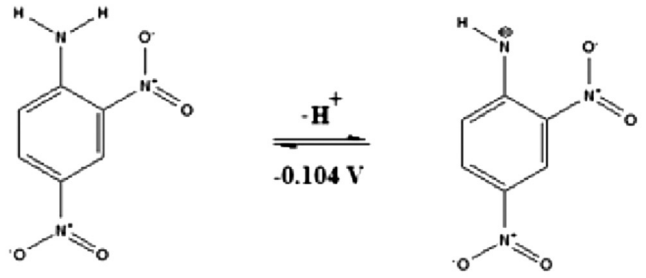

2,4-dinitroaniline **2,4-dinitroanilinium anion**

Reduction (Scan towards negative potential)

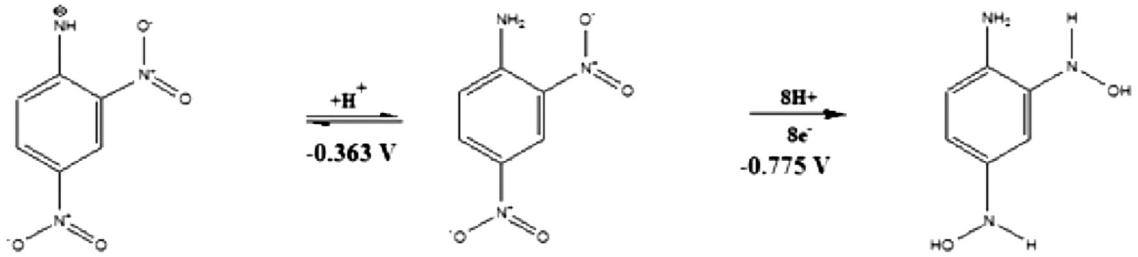

2,4-dinitroanilinium anion **2,4-dinitroaniline** **2,4-bishydroxylamine aniline**

In Alkali medium the following equilibrium exist as

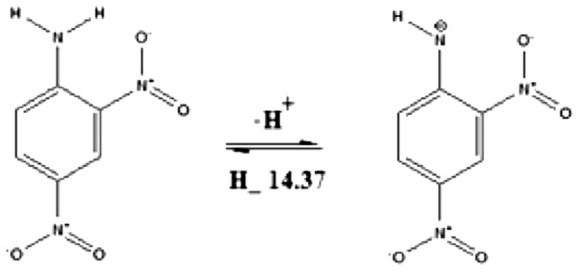

2,4-dinitroaniline **2,4-dinitroanilinium anion**

Reduction (Scan towards negative potential)

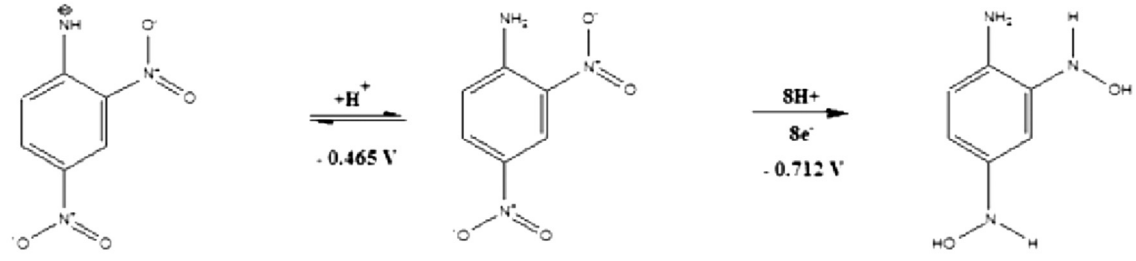

2,4-dinitroanilinium anion **2,4-dinitroaniline** **2,4-bishydroxylamine aniline**

Scheme 5. Reaction mechanism of 2,4-DNA in pH ~ 7 and H_14.37 buffer solutions at glassy carbon electrode.

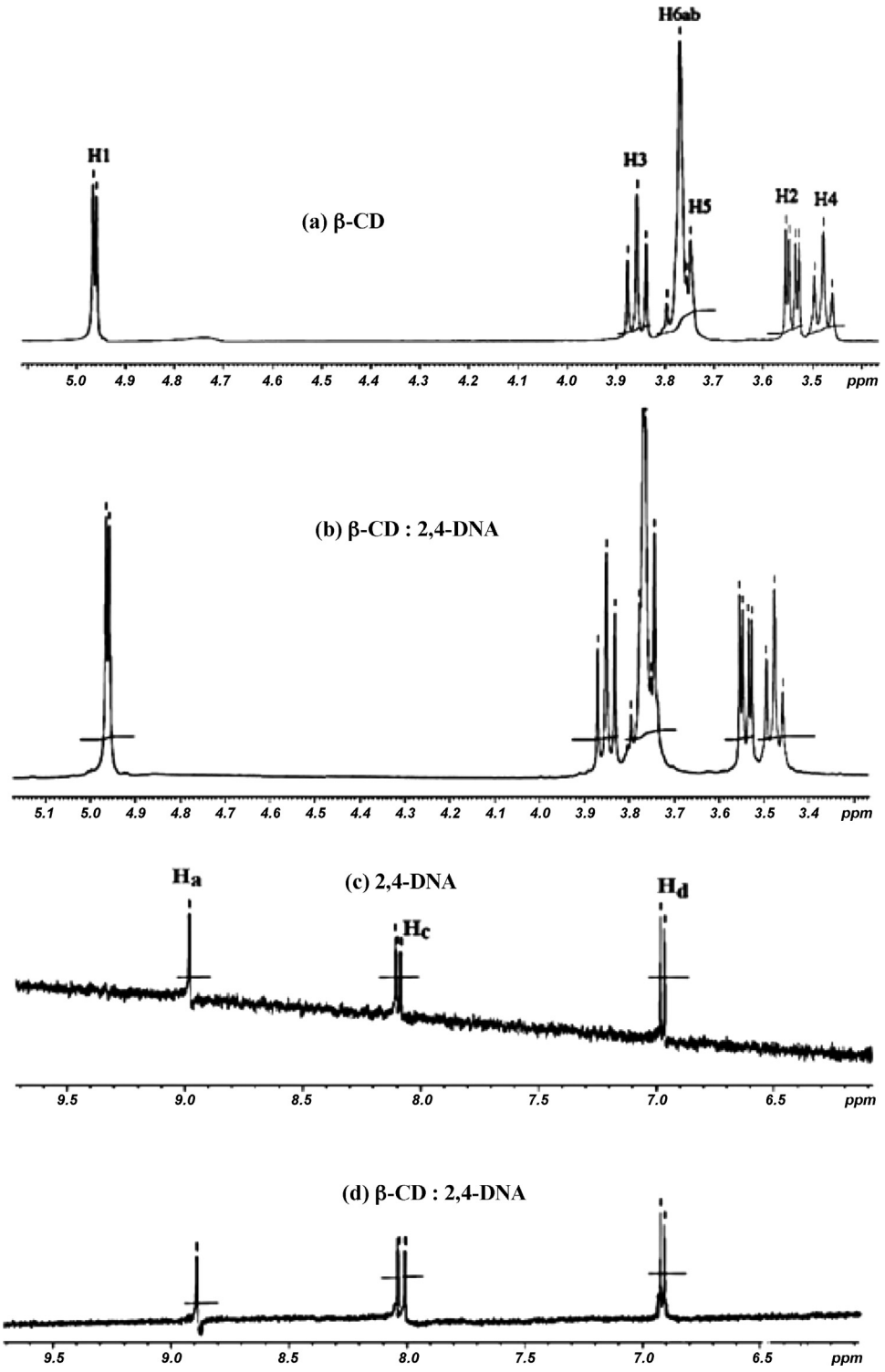

Fig. 4. 1H NMR spectra of (a) β-CD, (b) solid complex (chemical shift of β-CD); (c) 2,4-DNA, (d) inclusion complex (chemical shift of 2,4-DNA).

where I_G is the reduction peak current of the guest molecule of 2,4-DNA, and I_{HG} is the reduction peak current of inclusion complex of 2,4-DNA:β-CD. $I_{HG} - I_G$ is the difference between the reduction peak current of the inclusion complex and 2,4-DNA. ΔI is the difference between the molar peak current coefficient of the inclusion complex and 2,4-DNA. The $[2,4\text{-DNA}]_0$ and $[\beta\text{-CD}]_0$ are the initial concentration of 2,4-DNA and β-CD, respectively.

Plotting of $[1/I_{HG} - I_G]$ verses $1/[\beta\text{-CD}]$ gives a straight line for both pH solutions as shown in Fig. S2. Good linear correlations were obtained ($r = 0.9501$, 0.9228 for H_14.37 and pH ~ 7 respectively), its confirm that the formation of a 1:1 inclusion complex for both pH (H_14.37 and pH ~ 7) solutions. This plot of K was evaluated from the intercept and slope value, the binding constant values for 2,4-DNA: β-CD is 11.8 $M^{-1}$and 12 M^{-1} in H_14.37 and

Table 5
^{1}H NMR chemical shifts of β-CD and 2,4-DNA in free and complexed state determined In D_2O at 300 K.

Name of the substance	Protons	Free δ (ppm)	Complex δ (ppm)	$\Delta\delta$
β-CD	H_1	4.966	4.965	−0.001
	H_2	3.554	3.555	−0.001
	H_3	3.877	3.855	−0.022
	H_4	3.535	3.528	−0.007
	H_5	3.748	3.734	−0.014
	H_6	3.797	3.796	−0.001
2,4-DNA	H_a	8.982	8.908	−0.074
	H_c	8.105	8.086	−0.019
	H_d	6.982	6.905	−0.077

pH ~ 7 respectively. These values indicate that 2,4-DNA molecule is encapsulated in the β-CD cavity to form an inclusion complex.

3.6. ^{1}H NMR spectrum

The formation of the solid inclusion complex can be analyzed from ^{1}H NMR spectra (Chen, Diao, & Zhang, 2006). Fig. 4 showed the typical ^{1}H NMR spectra of (a) β-CD, (b) solid inclusion complex of 2,4-DNA with β-CD (chemical shift changes with β-CD), (c) 2,4-DNA and (d) solid inclusion complex (chemical shift changes with 2,4-DNA). The values of chemical shifts, δ for different protons in a β-CD with solid inclusion complex and 2,4-DNA with solid inclusion complex were listed in Table 5. It can be seen from the ^{1}H NMR that in solid inclusion complex, a great upfield shift was occurring for H_3 and H_5 protons, which locate in the nano hydrophobic cavity of β-CD (Scheme 6b). The changes of chemical shift ($\Delta\delta$) of H_3 and H_5 suggested that the 2,4-DNA monomer encapsulated into the nano hydrophobic cavity of β-CD. The phenyl ring of 2,4-DNA made the signals of β-CD protons (H_3 and H_5) upfield shift. On the contrary, the chemical shifts of H_1, H_2, H_4, and H_{6ab}, which are on the outer surface of β-CD and the narrow opening of β-CD (Scheme 6b), which were only slightly affected by the guest molecule. Similarly, the chemical shifts of H_a, H_b and H_c of 2,4-DNA (Scheme 4c) are located in the nano hydrophobic cavity of β-CD was also moved in upfield significantly, because when 2,4-DNA monomer entered into the nano hydrophobic cavity of β-CD, the change of the micro-environment of 2,4-DNA protons leaded the phenyl ring protons moved upfield shift. The significant distinguish for these ^{1}H NMR spectra strongly confirmed that the solid inclusion complex formation.

3.6.1. ROESY NMR (2D)

The 2D ROESY NMR is a powerful technique for investigation of inter and intra molecular interactions. The chemical shift changes were shown by H_a, H_c and H_d protons of aromatic (hydrophobic part) moiety (Sohajda et al., 2009) of 2,4-DNA may play a major role in the inclusion process. To verify this hypothesis, 2D ROESY NMR spectra were recorded. The presence of NOE cross-peaks between protons of two different species in 2D ROESY spectrum is an indication that they are in spatial contact through space within the cavity of β-CD.

Fig. 5 shows the 2D spectrum of 2,4-DNA:β-CD system, two groups of intermolecular NOE cross-peaks were observed. In the complex of 2,4-DNA:β-CD the first peak was assigned to the interaction between the H_3 protons of the β-CD with ortho positioned protons of the 2,4-DNA. The other peak was assigned to the interaction between the H_5 protons of the β-CD with meta positioned protons of the 2,4-DNA. In all cases the interaction of 2,4-DNA with internal protons of the β-CD was observed. In addition the H_{6ab} protons of the β-CD were not affected by the inclusion process. From this result we can confirm that 2,4-DNA was included into the β-CD cavity via wider rim. From the above fact the 2,4-DNA interact with β-CD through space contact, not by bonding.

3.7. FT-IR spectral studies

The solid inclusion complex formation has been characterized by FT-IR spectroscopy, because the bands resulting from the included part of the guest molecule are generally shifted or their intensities altered. Fig. 6 is the FT-IR spectra of (a) β-CD, (b) 2,4-DNA, (c) solid inclusion complex of 2,4-DNA. From

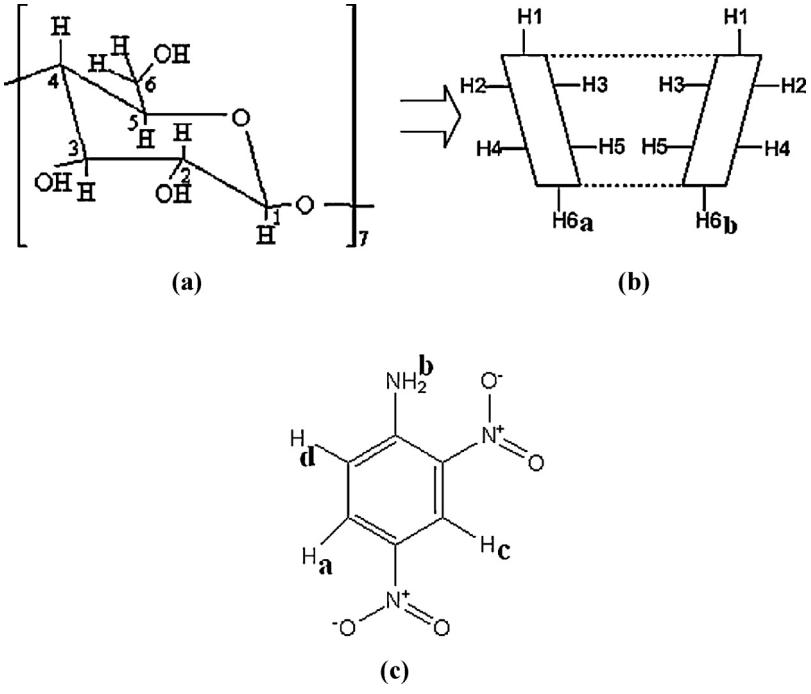

Scheme 6. (a) The stereo-configuration, (b) truncated-cone of β-CD and (c) 2,4-DNA.

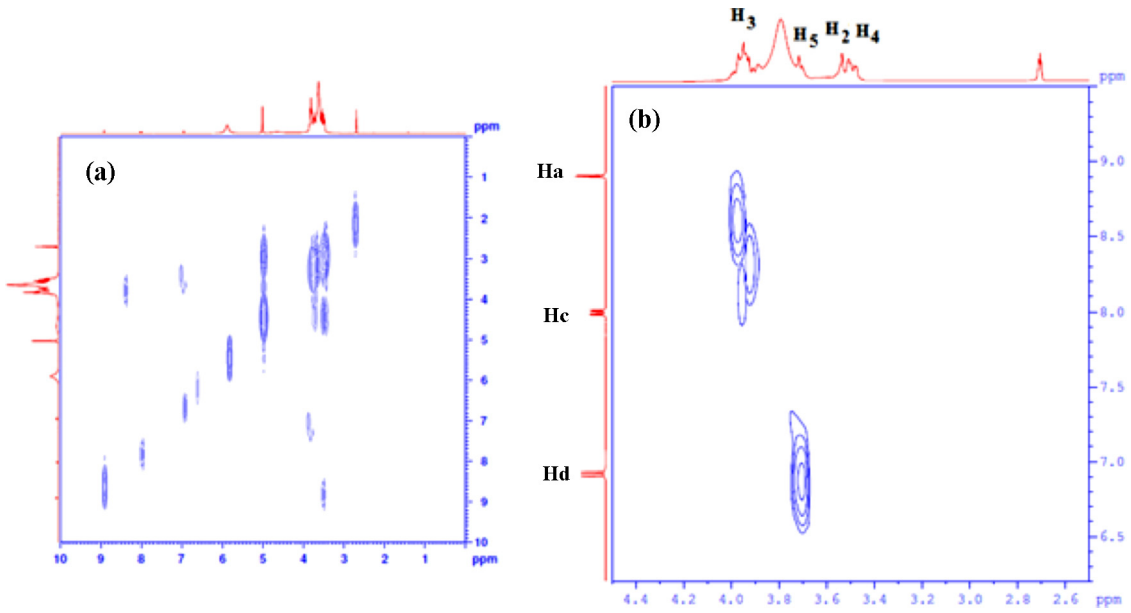

Fig. 5. 2D ROESY spectrum of inclusion complex of (a) 2,4-DNA:β-CD and (b) Partial counter plot of 2,4-DNA:β-CD in DMSO at 300 K.

the Fig. 6 the two characteristic stretching of -NO_2 peaks were observed at 1585 cm^{-1}, 1332 cm^{-1}. These stretching bands were shifted to 1589 cm^{-1}, 1332 cm^{-1} and also the intensity of these peaks were reduced this is due to the nitro group of 2,4-DNA was present (included) in the nanocavity of β-CD. The characteristics stretching of C—N (—NH) appeared at 1257 cm^{-1} and its shifted to 1263 cm^{-1}, this is due to the phenyl ring of 2,4-DNA was present in the nanocavity of the β-CD. The stretching band of C—N (—NO_2) group appeared at 833 cm^{-1} and it shifted to 835 cm^{-1} and also its intensity was reduced, because of the nitro group was entrapped into the nanocavity of β-CD. The stretching vibration of —C=C— appeared at 1627 cm^{-1} and it shifted to 1629 cm^{-1}, and its intensity also reduced, due to the hydrophobic part of the benzene ring to 2,4-DNA was included into the nanocavity of the β-CD. As can be seen above discussions it can be concluded that of 2,4-DNA molecule was included in β-CD cavity.

3.8. Powder X-ray diffraction pattern

The lack of crystallinity is an added evidence for the formation of inclusion complex (Williams, Mahaguna, & Sriwongjanya, 1998). Fig. 7 show the XRD patterns for guest (2,4-DNA), host (β-CD) and their solid inclusion complex systems were prepared by co-precipitation techniques at a molar ratio of 1:1. The powder X-ray diffraction pattern of 2,4-DNA (Fig. 7a) revealed that several sharp high intensity peaks at different diffraction angles (2θ) of 13.7, 14.2, 18.5, 19.6, 20.6, 23.3, 28.0, 28.9 and 31.3 suggesting that the 2,4-DNA existed as crystalline nature. The β-CD (Fig. 7b) showed a crystalline diffractogram, while a diffuse halo-pattern was recorded for 2,4-DNA-β-CD (Fig. 7c) demonstrating its amorphous nature. The diffraction patterns of the investigated in the solid inclusion complex correspond to the correct position of those of the pure components. The lower intensities of the diffraction peaks indicate that the particle sizes were reduced during complex

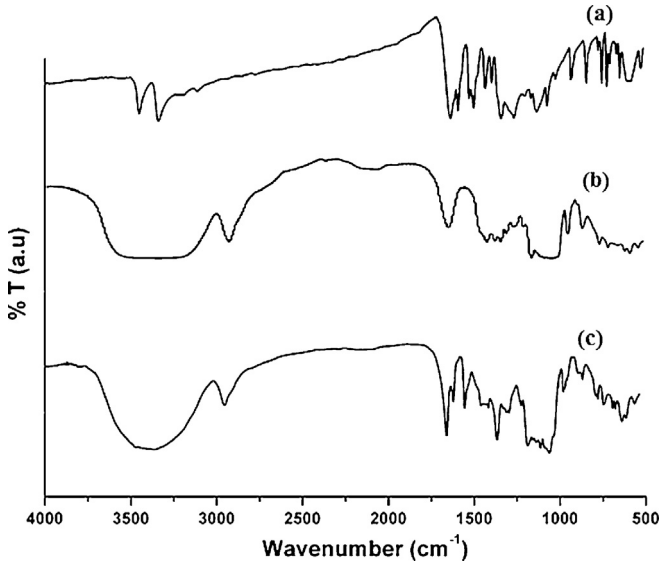

Fig. 6. FT-IR spectra of (a) 2,4-DNA, (b) β-CD and (c) inclusion complex of 2,4-DNA:β-CD complex in KBr pellet.

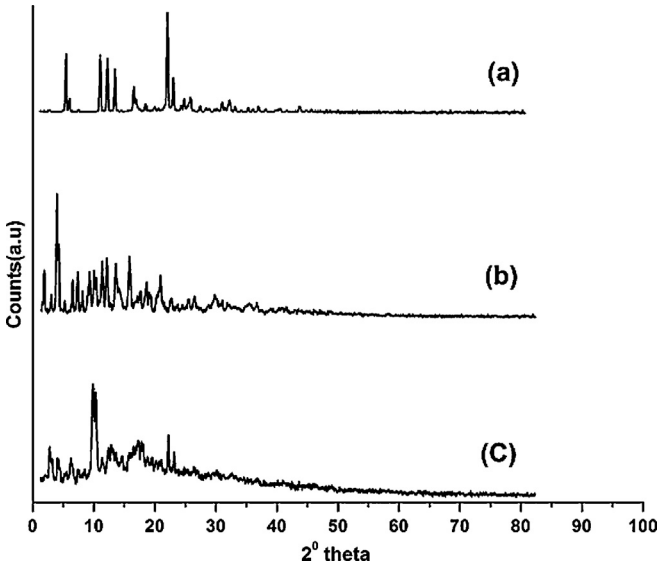

Fig. 7. Powder X-ray diffraction pattern of (a) 2,4-DNA, (b) β-CD and (c) inclusion complex of 2,4-DNA:β-CD.

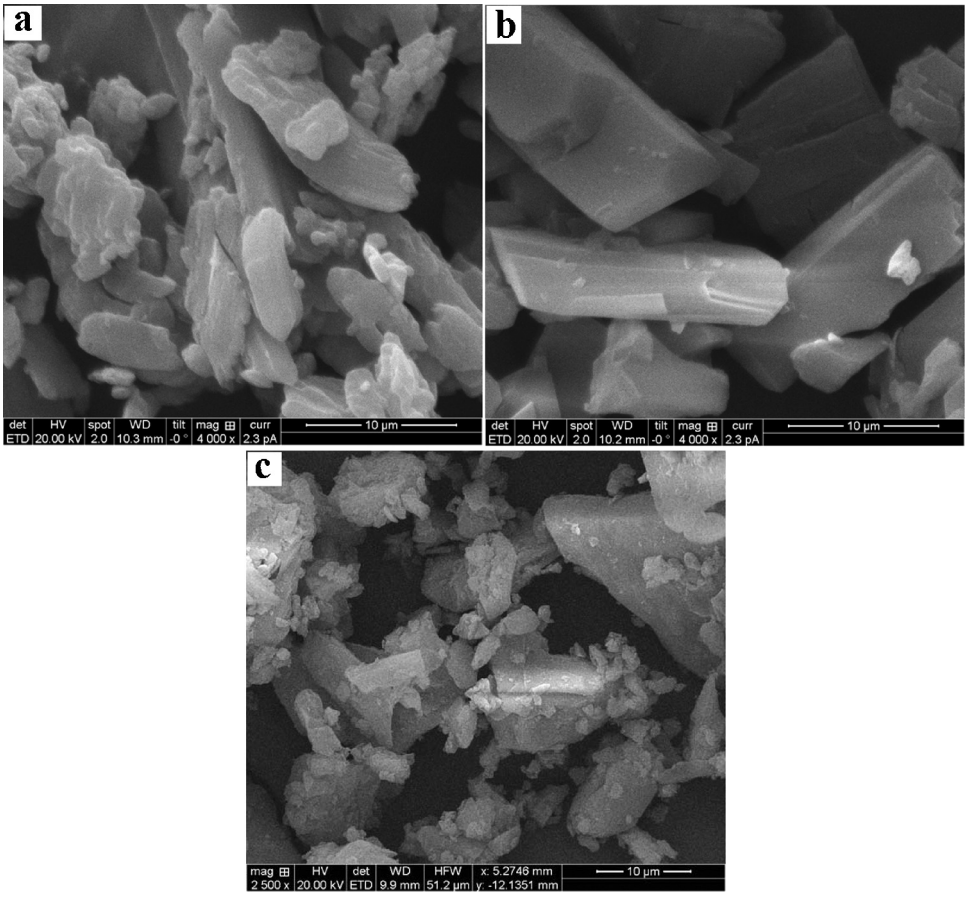

Fig. 8. Scanning electron microscope photographs (Pt. coated) of (a) 2,4-DNA (b) inclusion complex of 2,4-DNA:β-CD and (c) β-CD.

preparation in solution phase of the pure crystalline components. Few of diffraction peaks of 2,4-DNA was matched with those off β-CD was evident. A typical diffuse pattern indicating the entirely amorphous nature of 2,4-DNA in complexed state.

3.9. Scanning electron microscope morphological observations

Scanning electron microscope (SEM) is well suited for visualizing the surface texture of the deposited film. The SEM analysis is ideal for measuring the surface roughness and for visualizing the surface texture of the substance. First we observed surface morphological structure of (a) 2,4-DNA,(b) β-CD (Fig. 8) by SEM, and then we also observed the surface morphological structure of (c) solid inclusion complex (Fig. 8c). These pictures clearly elucidated the difference of each other. Modification of crystals can be assumed as a proof of the formation of a solid inclusion complex with the nano hydrophobic cavity of β-CD.

4. Conclusions

(i) The ground state acidity constant (pK_a) value for the prototropic species of 2,4-DNA was calculated by spectrophotometricaly, (ii) 2,4-DNA forms a 1:1 inclusion complex with β-CD in neutral and alkali conditions, (iii) Prototropic reactions in β-CD medium indicates in neutral (NH_2) and monoanion ($-NH^{(-)}$ deprotanated group) present in the above the β-CD rim (iv) The electrochemical studies also confirmed the formation of the inclusion complex in both pH∼(7 and H_14.37), (v) FT-IR, ^1H NMR, 2D ROESY NMR, XRD and SEM results suggest that 2,4-DNA formed an inclusion complex with the nano hydrophobic cavity of β-CD, (vi) The energetically favorable complex was obtained by molecular docking studies and it was good correlation with the inclusion model predicted through experimental investigations.

Acknowledgements

One of the authors K. Srinivasan acknowledges to UGC-BSR for providing Research Fellowship for Science Meritorious (AU/UGC-BSR/IC/1069/2011) student and we are thankful to SAIF IIT Madras for utilizing the ^1H NMR spectra facility.

Appendix A. Supplementary data

Supplementary data associated with this article can be found, in the online version, at http://dx.doi.org/10.1016/j.carbpol.2014.01.091.

References

Armson, A., Sargent, K., MacDonald, L. M., Finn, M. P., Thompson, R. C. A., & Reynoldson, J. A. (1999). A comparison of the effects of two dinitroanilines against Cryptosporidium parvum in vitro and in vivo in neonatal mice and rats. *FEMS Immunology and Medical Microbiology*, *26*(2), 109–111.

Ayala, P. C., El-Din, M. G., & Smith, D. W. (2010). Kinetics and mechanism of the degradation of two pesticides in aqueous solutions by ozonation. *Chemosphere*, *78*(5), 557–562.

Benbow, J. W., Bernberg, E. L., Korda, A., & Mead, J. R. (1998). Synthesis and Evaluation of Dinitroanilines for Treatment of Cryptosporidiosis. *Antimicrobial Agents and Chemotherapy*, *42*(2), 339–343.

Benesi, H. A., & Hildebrand, J. H. (1949). A Spectrophotometric Investigation of the Interaction of Iodine with Aromatic Hydrocarbons. *Journal of the American Chemical Society*, *71*, 2703–2707.

Chen, M., Diao, G., & Zhang, E. (2006). Study of Inclusion complex of β-cyclodextrin and nitrobenzene. *Chemosphere*, *63*, 522–529.

Choi, S. H., Nyongryu, E., Ryoo, J., & Pillee, K. (2001). FT-Raman Spectra of o-, m-, and p-Nitrophenol Included in Cyclodextrins. *Journal of Inclusion Phenomena and Macrocyclic Chemistry*, *40*(4), 271–274.

Connolly, M. L. (1983a). Analytical molecular surface calculation. *Journal of Applied Crystallography*, *16*, 548–558.

Connolly, M. L. (1983b). Solvent-Accessible Surfaces of Proteins and Nucleic Acids. *Science*, *221*(4612), 709–713.

Dimou, A. D., Sakkas, V. A., & Albanis, T. A. (2004). Photodegradation of trifluralin in natural waters and soils: degradation kinetics and influence of organic matter. *International Journal of Environmental Analytical Chemistry*, *84*(1-3), 173–182.

Do Nascimento, G. M., Da Silva, J. E. P., De Torresi, S. I. C., Santos, P. S., & Temperini, M. L. A. (2002). Spectroscopic characterization of the inclusion compound formed by polyaniline and beta-cyclodextrin. *Molecular Crystals and Liquid Crystals*, *374*(1), 53–58.

Duhovny, D. S., Inbar, Y., Nussinov, R., & Wolfson, H. J. (2005). PatchDock and SymmDock: servers for rigid and symmetric docking. *Nucleic Acids Research*, *33*, 363–367.

Harada, A., Nishiyama, T., Kawaguchi, Y., Okada, M., & Kamachi, M. (1997). Preparation and Characterization of Inclusion Complexes of Aliphatic Polyesters with Cyclodextrins. *Macromolecules*, *30*(23), 7115–7118.

Jorgenson, M. J., & Hartter, D. R. (1963). A Critical Re-evaluation of the Hammett Acidity Function at Moderate and High Acid Concentrations of Sulfuric Acid. New H_0 Values Based Solely on a Set of Primary Aniline Indicators. *Journal of the American Chemical Society*, *85*(7), 878–883.

Kataoka, H. (1996). Derivatization reactions for the determination of amines by gas chromatography and their applications in environmental analysis. *Journal of Chromatography A*, *733*, 19–34.

Kearney, P. C., Isensee, A. R., & Koktson, A. (1977). Distribution and degradation of dinitroaniline herbicides in an aquatic ecosystem. *Biochemistry and Physiology*, *7*(3), 242–248.

Loukas, Y. L., Jayasekera, P., & Gregoriadis, G. (1995). Novel liposome-based multicomponent systems for the protection of photolabile agents. *International Journal of Pharmaceutics*, *117*(1), 85–94.

Loukas, Y. L., Vraka, V., & Gregoriadis, G. (1996). Use of a nonlinear least-squares model for the kinetic determination of the stability constant of cyclodextrin inclusion complexes. *International Journal of Pharmaceutics*, *144*(2), 225–231.

Rekharsky, M. V., & Inoue, Y. (1998). Complexation Thermodynamics of Cyclodextrins. *Chemical Reviews*, *98*(5), 1875–1918.

Schneider, H. J., Hacket, F., & Rudiger, V. (1998). NMR Studies of Cyclodextrins and Cyclodextrin Complexes. *Chemical Reviews*, *98*(5), 1755–1786.

Shuai, X. T., Porbeni, F. E., Wei, M., Shin, I. D., & Tonelli, A. E. (2001). Formation of and Coalescence from the Inclusion Complex of a Biodegradable Block Copolymer and α-Cyclodextrin: A Novel Means To Modify the Phase Structure of Biodegradable Block Copolymers. *Macromolecules*, *34*(21), 7355–7361.

Sohajda, T., Beni, S., Varga, E., Ivanyi, R., Racz, A., Szente, L., & Noszal, B. (2009). Characterization of aspartame–cyclodextrin complexation. *Journal of Pharmaceutical and Biomedical Analysis*, *50*, 737–745.

Stalin, T., Srinivasan, K., Kayalvizhi, K., & Sivakumar, K. (2011). Study of inclusion complex of β-cyclodextrin and diphenylamine:Photophysical and electrochemical behaviors. *Spectrachimica Acta Part A: Molecular and Biomolecular Spectroscopy*, *79*, 169–178.

Stalin, T., Srinivasan, K., Vaheethabanu, J., & Manisankar, P. (2011). Study of inclusion complex of β-cyclodextrin and Ortho-Anisidine; photophysical and electrochemical behaviors. *Journal of Molecular Structure*, *987*(1–3), 214–224.

Szejtli, J. (1998). Introduction and general overview of cyclodextrin chemistry. *Chemical Reviews*, *98*(5), 1743–1753.

Wang, S., & Arnold, W. A. (2003). Abiotic reduction of dinitroaniline herbicides. *Water Research*, *37*(17), 4191–4201.

Williams, R. O., Mahaguna, V., & Sriwongjanya, M. (1998). Characterization of an inclusion complex of Cholesterol and hydroxypropyl β-cyclodextrin. *European Journal of Pharmaceutics and Biopharmaceutics*, *46*, 355–360.

Xiang, G. H., Tong, C. L., & Lin, H. Z. (2007). Nitroaniline Isomers Interaction with Bovine Serum Albumin and Toxicological Implications. *Journal of Fluorescence*, *17*(5), 512–521.

Xifeng, G., Jin, L., Weidong, Z., Qingjiang, W., Pingang, H., & Yuzhi, F. (2006). Separation and determination of nitroaniline isomers by capillary zone electrophoresis with amperometric detection. *Talanta*, *69*(1), 121–125.

Xu, L., Liu, S. M., Wu, C. T., & Feng, Y. Q. (2004). Separation of positional isomers by cucurbit[7]uril-mediated capillary electrophoresis. *Electrophoresis*, *25*(18-19), 3300–3306.

Yagil, G. (1967). The Effect of Ionic Hydration on Equilibria and Rates in Concentrated Electrolyte Solutions. III. The H- Scale in Concentrated Hydroxide Solutions. *Journal of Physical Chemistry*, *71*, 1034–1044.

Zhang, C., Vasmatzis, G., Cornette, J. L., & DeLisi, C. (1997). Determination of atomic desolvation energies from the structures of crystallized proteins. *Journal of Molecular Biology*, *267*(3), 707–726.

Zhang, L., Lerner, S., Rustrum, W. V., & Hofman, G. A. (1999). Electroporation-mediated topical delivery of vitamin C for cosmetic applications. *Bioelectrochemistry and Bioenergetics*, *48*(2), 453–461.